



Article

Non-Noble-Metal Mono and Bimetallic Composites for Efficient Electrocatalysis of Phosphine Oxide and Acetylene C-H/P-H Coupling under Mild Conditions

Maxim V. Tarasov , Olga D. Bochkova , Tatyana V. Gryaznova, Asiya R. Mustafina and Yulia H. Budnikova *

Arbuzov Institute of Organic and Physical Chemistry, FRC Kazan Scientific Center of RAS, Arbuzov Str. 8, 420088 Kazan, Russia

* Correspondence: olefindirector@gmail.com

Abstract: The present work describes an efficient reaction of electrochemical phosphorylation of phenylacetylene controlled by the composition of catalytic nanoparticles based on non-noble-metals. The sought-after products are produced via the simple synthetic protocol based on room temperature, atom-economical reactions, and silica nanoparticles (SNs) loaded by one or two d-metal ions as nanocatalysts. The redox and catalytic properties of SNs can be tuned with a range of parameters, such as compositions of the bimetallic systems, their preparation method, and morphology. Monometallic SNs give phosphorylated acetylene with retention of the triple bond, and bimetallic SNs give a bis-phosphorylation product. This is the first example of acetylene and phosphine oxide C-H/P-H coupling with a regenerable and recyclable catalyst.

Keywords: electrochemistry; composite; mono and bimetallic catalyst; acetylene; phosphonation



Citation: Tarasov, M.V.; Bochkova, O.D.; Gryaznova, T.V.; Mustafina, A.R.; Budnikova, Y.H. Non-Noble-Metal Mono and Bimetallic Composites for Efficient Electrocatalysis of Phosphine Oxide and Acetylene C-H/P-H Coupling under Mild Conditions. *Int. J. Mol. Sci.* **2023**, *24*, 765. <https://doi.org/10.3390/ijms24010765>

Academic Editor: Albert Poater

Received: 20 December 2022

Revised: 28 December 2022

Accepted: 29 December 2022

Published: 1 January 2023



Copyright: © 2023 by the authors. Licensee MDPI, Basel, Switzerland. This article is an open access article distributed under the terms and conditions of the Creative Commons Attribution (CC BY) license (<https://creativecommons.org/licenses/by/4.0/>).

1. Introduction

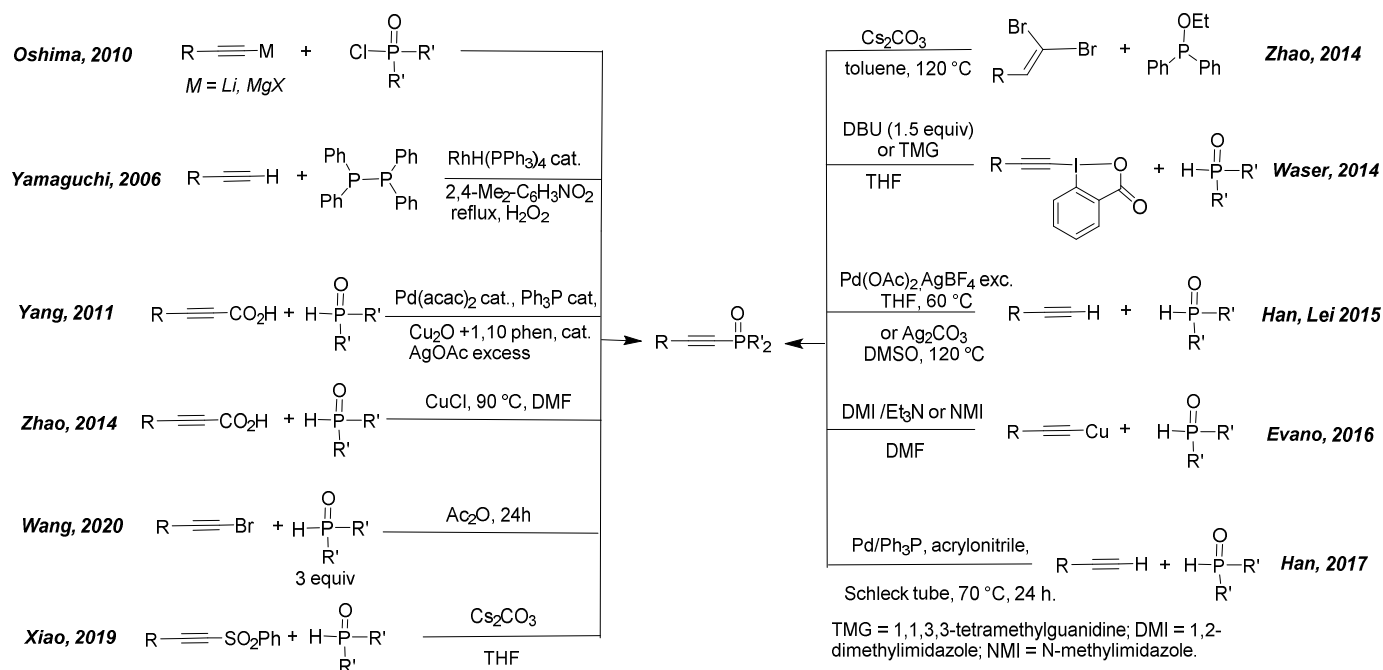
In recent years, the development of new efficient catalytic systems based on inexpensive non-noble metals has been an important component of green chemistry [1–3]. Bioinspired tandem catalysis based on bimetallic structures has opened a new dimension of efficient catalytic systems, surpassing traditional catalytic methods of organic synthesis, often reducing the number of stages, reaction time and facilitating process conditions [4–9]. In addition, the growing demand for environmentally friendly and economical synthetic procedures is also driving the development of multiple catalytic one-pot conversions in order to obtain the desired product in the most efficient manner. In this regard, mono- and bimetallic heterogeneous, nanoheterogeneous catalysts are excellent candidates for selective transformations, with the possibility of regeneration and easy separation of the catalyst from the reaction mixture [10,11].

In bimetallic catalyst systems, two different metals can catalyze two or more different types of reactions or steps, with some synergy between the two metals. Thus, the use of bimetallic catalyst systems can result in an overall increase in reactivity and selectivity over their monometallic counterparts. Stability and adaptability appear to be important factors in the synthesis of these bimetallic catalysts, for which the nature of the support matrix or ligand may play a decisive role. In electrochemical processes, such nanoheterogeneous catalytic structures are used as sensors [12,13], in electrosynthesis of practically significant complex molecules [14–22], for activation of CO₂, N₂, and other small molecules [23,24].

Substituted alkynes and alkenes are fundamental structural motifs that are widely distributed in natural products, bioactive molecules, and functional materials. They serve as universal synthetic precursors and/or intermediates in organic transformations [25–38]. Despite the long history of the functionalization of alkynes, the search for new ways and catalysts is very relevant. For example, a new strategy has been proposed for multi-metal-catalyzed (Cu, Ni, Ag) oxidative radical alkylation with terminal alkynes as

Sonogashira-type alkynylation for C(sp³)-C(sp) bond formation at 80–100 °C, however, the regeneration of the catalytic components is impossible in this case [26].

Phosphorylation of acetylenes is an important way to obtain practically significant ligands, flame retardants, biologically active compounds, for example, the progesterone receptor antagonist [27]. Depending on the conditions and reagents, the products may contain both a carbon-carbon triple bond [28–42] and a double [43–46] or single [47–49] bonds upon hydrophosphination. The classical routes to phosphorus-substituted alkynes are mostly based on elimination reactions from the corresponding vinylhalide/pseudohalide derivatives or the reaction of a metal acetylide with a halophosphine or a derivative [33] (Scheme 1). Despite the success of their synthesis, most reactions are carried out under harsh and hazardous conditions, techniques include elevated temperatures [36,38,39], excess oxidizing agents and expensive radical initiators (such as DBU [28,32]), catalyst metals, primarily expensive palladium, rhodium and silver [34,35,39,40,42,44], the latter is in excess in many cases, are often based on sulfonyl [29], halogen [32,33,37] and other derivatives [32,35,36,38,41] (Scheme 1).



Scheme 1. Reported routes of acetylene derivatives phosphorylations: Xiao, 2019 [29]; Waser, 2014 [32]; Oshima, 2010 [33]; Yamaguchi, 2006 [34]; Yang, 2011 [35]; Zhao, 2014 [36]; Wang, 2020 [37]; Zhao, 2014 [38]; Han, 2015 [39]; Lei, 2015 [40]; Evano, 2016 [41]; Han, 2017 [42].

Recoverable and recyclable catalytic systems for these transformations are not described.

In this regard, the development of an efficient and environmentally benign method for the direct construction of C(sp, sp², sp³)-P bonds through C-H/P-H coupling of acetylenes and phosphine oxides under noble metal- and oxidant-free conditions is still highly desirable.

The rationale for choosing copper and cobalt as metal components of catalysts is associated with their availability and activity in various phosphorylation reactions, primarily through unsaturated bonds. In particular, the works [30,31,46,48,50–52] exemplify the copper- and cobalt-catalyzed reactions correspondingly.

Silica nanoparticles (SNs) were widely applied as convenient nanobeads for different metal ions and complexes. Moreover, metal ions or complexes can be incorporated into SNs through either (1) localization within silica confinement or (2) surface adsorption. These two ways of incorporation allow tuning and exposure of the doped metal ions to a bulk of solution. The present work introduces a synthetic procedure to incorporate cobalt, copper, and iron ions into SNs, thus, producing original mono- and bimetallic nanomaterial for the

use as nanocatalyst of the reductive coupling of phenylacetylene and diphenylphosphine oxide through the C-H/P-H reaction. It is worth noting that SNs serve as carriers of metal ions, thus, preventing their leaching and further undesirable transformations. The backgrounds of the bimetallic nanoparticles are the previously developed synthetic procedures allowing the encapsulation of both Co^{II} ions and Co^{III} complexes into the silica nanoparticles (SNs) [13,20]. It will be shown that the catalytically active form of the nanocatalyst is generated electrochemically at the cathode, and the nature (mono or bimetallic) of the catalyst is of great impact on the products of the reaction.

2. Results and Discussion

2.1. Synthesis of Nanocomposite Catalytic Systems

The composite SNs were synthesized in the framework of core-shell morphology, where metal ions were incorporated within silica spheres through either doping or adsorption procedures. The localization of metal salts or complexes within silica confinement can be realized through their addition into the synthetic mixture, while the incorporation through surface adsorption can be performed under the post-treating of the synthesized SNs. Both microemulsion water-in-oil and Stober procedures are commonly applied techniques for the synthesis of SNs. It is worth noting that the use of either microemulsion or Stober techniques allows controlling both the size and porosity of the silica spheres [53]. The addition of metal complexes or metal ions into the synthetic mixture results in their encapsulation into silica spheres, thus, resulting in the composite SNs. It is worth noting that the Co^{III} ions are incorporated in the form of kinetically inert $[\text{Co}(\text{dipy})_3]^{3+}$ complexes. Thus, their inner-sphere environment remains unchanged after the synthetic procedure [20], resulting in the composite SNs designated as $\text{Co}^{\text{III}}@\text{SN}_{50}$ and $\text{Co}^{\text{III}}@\text{SN}_{120}$, where 50 and 120 is their size in nanometers. The applied synthetic procedures are described in detail in the Exp. Section and schematically represented in Figure 1. The Co^{III} -content is greater in $\text{Co}^{\text{III}}@\text{SN}_{50}$ vs. $\text{Co}^{\text{III}}@\text{SN}_{120}$, which is the agreement with the previously reported tendency [20]. The doping of Co^{II} ions into the SN_{50} was performed through the microemulsion synthetic procedure [13].

As it has been previously demonstrated, the high activity of silanol groups is the reason for their complexation with d-metal ions, which provides a main driving force of the specific adsorption of d-metal ions [54,55]. The stirring of the empty SN_{50} and SN_{120} in the aqueous solutions of Cu^{II} and Fe^{III} chlorides results in significant adsorption, which is evident from the Si:Cu(Fe) molar ratios in the SNs after their separation from the aqueous solutions and washing (Table 1).

Table 1. Si:Co:Cu or Si:Co:Fe Molar ratio by ICP-OES technique and ζ -potential values evaluated by DLS technique for different silica nanoparticles dispersion ($0.2 \text{ g}\cdot\text{L}^{-1}$).

Sample	Si:Co:Cu/Fe	ζ , mV ($\pm 5\%$)
SN_{50}	-	-36
SN_{120}	-	-35
$\text{SN}_{50}\text{-Cu}^{\text{II}}$	1:0:0.0067	-23
$\text{SN}_{120}\text{-Cu}^{\text{II}}$	1:0:0.0282	-27
$\text{SN}_{50}\text{-Fe}^{\text{III}}$	1:0:0.0250	-30
$\text{Co}^{\text{II}}@\text{SN}_{50}$	1:0.0068	-33
$\text{Co}^{\text{II}}@\text{SN}_{50}\text{-Cu}^{\text{II}}$	1:0.0063:0.0028	-31
$\text{Co}^{\text{III}}@\text{SN}_{50}$	1:0.0072	-33
$\text{Co}^{\text{III}}@\text{SN}_{120}$	1:0.0043	-44
$\text{Co}^{\text{III}}@\text{SN}_{50}\text{-Cu}^{\text{II}}$	1:0.0056:0.0056	-33
$\text{Co}^{\text{III}}@\text{SN}_{120}\text{-Cu}^{\text{II}}$	1:0.0013:0.0286	-23
$\text{Co}^{\text{III}}@\text{SN}_{50}\text{-Fe}^{\text{III}}$	1:0.0050:0.0820	-20

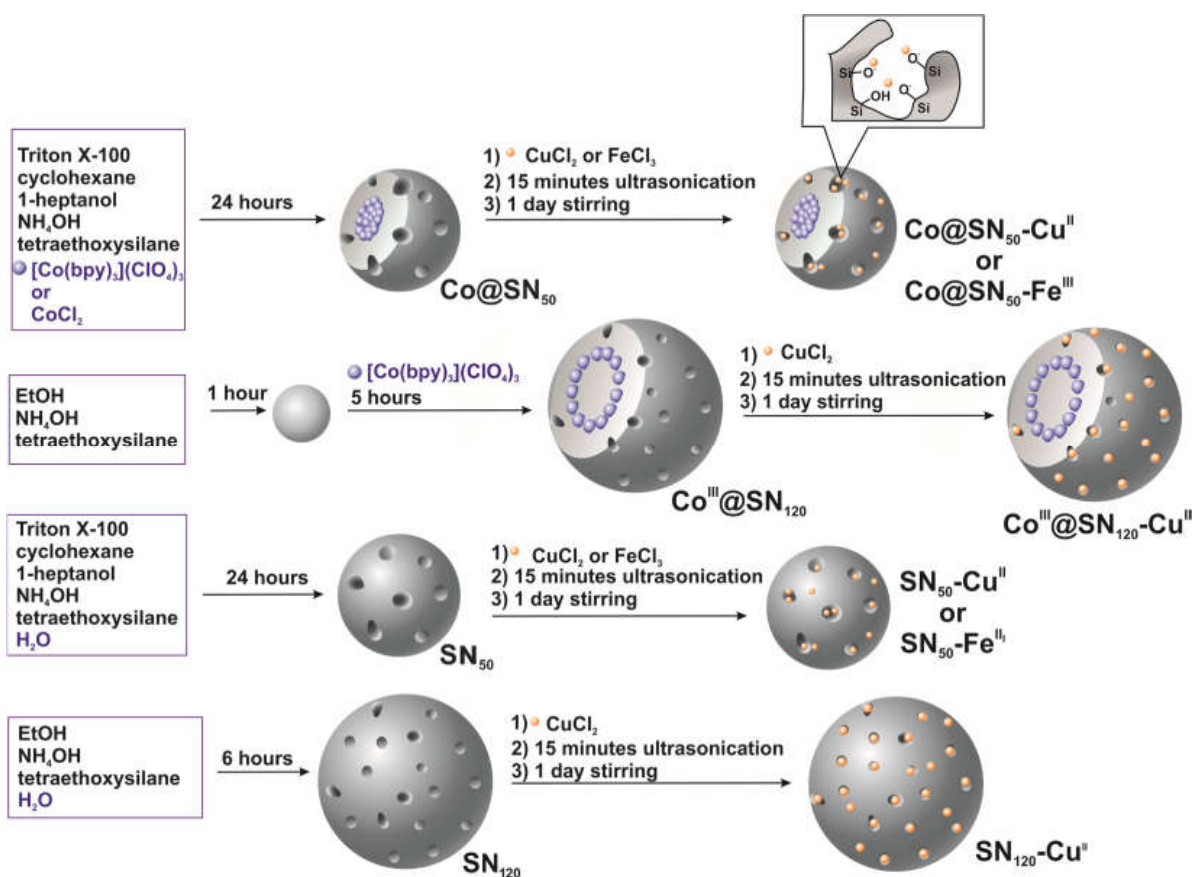


Figure 1. Schematic illustration of the synthesis of Co^{III}@SN₅₀, Co^{III}@SN₅₀-Cu^{II}(Fe^{III}), Co^{II}@SN₅₀, Co^{II}@SN₅₀-Cu^{II}, SN₅₀-Cu^{II}(Fe^{III}), Co^{III}@SN₁₂₀, Co^{III}@SN₁₂₀-Cu^{II}, SN₁₂₀-Cu^{II} through both doping and absorption procedures.

The composites Co^{III}@SN₅₀ and Co^{III}@SN₁₂₀ also demonstrate similar adsorption of both metal ions (Table 1). The metal ions incorporated through the adsorption technique are manifested by the bands in the diffuse reflectance spectra (Figure 2) at the wavelengths (800–900 nm and 400–550 nm) peculiar for the d-d transition of Cu^{II} and Fe^{III}, respectively [56].

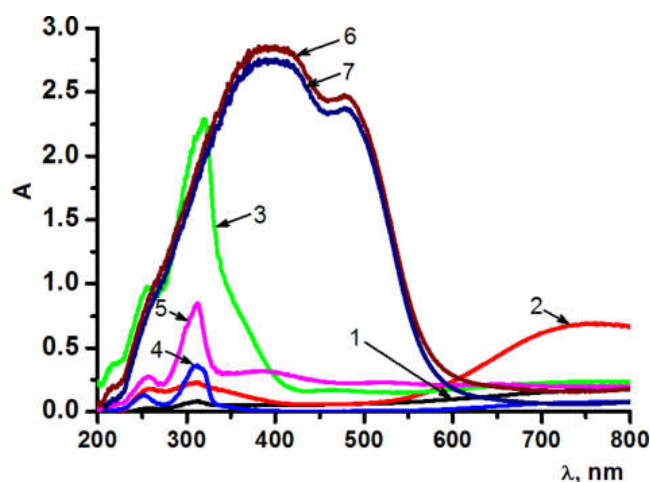


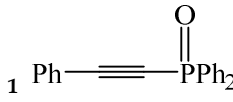
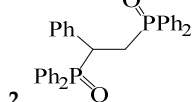
Figure 2. UV-Vis diffuse reflectance spectra of: 1—SN₅₀-Cu^{II}, 2—SN₁₂₀-Cu^{II}, 3—Co^{III}@SN₅₀-Cu^{II}, 4—Co^{III}@SN₁₂₀-Cu^{II}, 5—Co^{II}@SN₅₀-Cu^{II}, 6—SN₅₀-Fe^{III}, 7—Co^{III}@SN₅₀-Fe^{III}.

The DLS measurements of the aqueous colloids of the mono and bimetallic SNs are characterized by negative electrokinetic potential values (Table 1), which argues for the fact that the adsorbed metal ions exhibit rather deep penetration into the silica matrix (Figure 1). The values of the hydrodynamic radius and polydispersity index of the SNs represented in Table S1 indicate the similarity in the aggregation behavior of the bimetallic and monometallic SNs.

2.2. Electrocatalytic Phosphorylation of Phenylacetylene

The redox properties of the nanoparticles were studied using cyclic voltammetry (CV) on modified glassy carbon electrodes. Peaks of the corresponding metals are observed on the CVs (Table 2). The redox transitions of $\text{Cu}^{\text{II/I}}$, $\text{Fe}^{\text{III/II}}$, $\text{Co}^{\text{III/II}}$ bpy_n are usually reversible or quasi-reversible, which indicates the stabilization of the reduced forms of metals in a specific environment. The proximity of the first potentials of the reduction peaks of the metals included in the bimetallic nanoparticles leads to a complex shape of the peaks that cannot be resolved and accurately assigned (Figures S2–S8 in Supplementary Materials). Peak potentials are shown in Table 2.

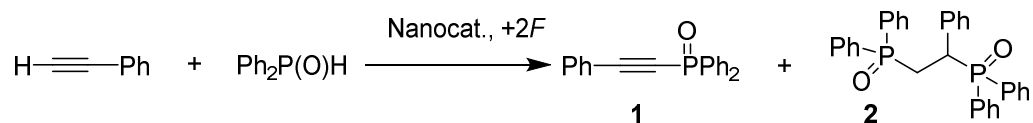
Table 2. Reduction peak potentials on nanoparticle-modified glassy carbon electrode. Products of $\text{Ph}_2\text{P}(\text{O})\text{H}$ and phenylacetylene (1:1) coupling, 2F, CH_3CN , Bu_4NBF_4 .

N	Catalysts	$-E_{\text{p}}^{\text{red}}, \text{V}$	Products, Yields Based on ^{31}P Spectra	
			1	2
				
1	$\text{Co}^{\text{III}}\text{-SN}_{50}$	−0.17, −1.37, −1.89	98 *	traces
2	$\text{Co}^{\text{III}}\text{-SN}_{50}\text{-Cu}^{\text{II}}$	−0.9 ^{small} , −1.41 ^{main} , −2.35	80 *	20
3	$\text{Co}^{\text{II}}\text{-SN}_{50}\text{-Cu}^{\text{II}}$	−1.37, −2.56	85	15
4	$\text{SN}_{50}\text{-Cu}^{\text{II}}$	−1.23, −2.08	99	traces
5	$\text{SN}_{120}\text{-Cu}^{\text{II}}$	−1.23, −2.08	76	24
6	$\text{SN}_{50}\text{-Fe}^{\text{III}}$	−1.85	97	3
7	$\text{Co}^{\text{III}}\text{-SN}_{50}\text{-Fe}^{\text{III}}$	−0.88 ^{small} , −1.45 ^{main} , −2.51	80	20

* mixture of two isomers.

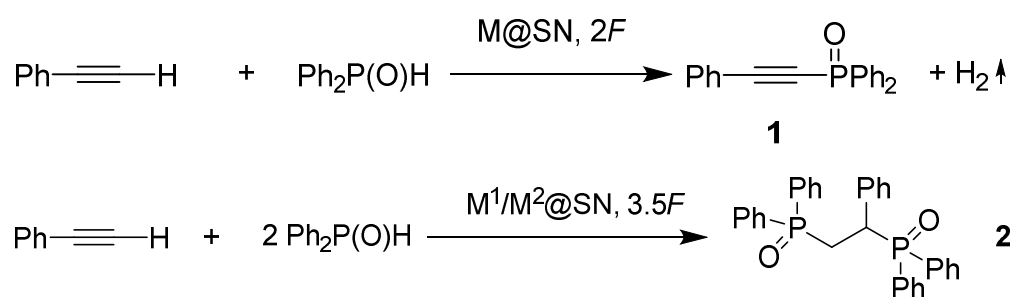
The studied nanoparticles were tested for catalytic activity in the phenylacetylene phosphorylation reaction of phenylacetylene with diphenylphosphine oxide under electroreductive conditions. The $\text{Ph}_2\text{P}(\text{O})\text{H}$ conversion was 100% in all cases.

Joint electrolysis of diphenylphosphine oxide with phenylacetylene (1:1) under electrochemical reduction conditions in the presence of the nanocatalyst at room temperature with a background electrolyte Et_4NBF_4 in the galvanostatic mode with the passage of 2F electricity proceeds with the formation of diphenyl(phenylethynyl)phosphine oxide (1) in the form of a mixture isomers and (1-phenylethane-1,2-diyl)bis(diphenylphosphine oxide) (2) (Scheme 2, Table 2). The cathode potential in all cases was −1.5–1.6 V when passing 2 F of electricity and increased to −1.9 V with further electrolysis. Monitoring of the process by ^{31}P NMR spectra showed that after 1F electricity, product (1) and the residual amount of the precursor $\text{Ph}_2\text{P}(\text{O})\text{H}$ are present in the solution. After the passage of 2 F electricity, product (2) precipitated from the reaction mixture, and the ^{31}P NMR spectrum of the solution contained only the signal of compound (1) and no traces of the starting $\text{Ph}_2\text{P}(\text{O})\text{H}$.



Scheme 2. C-H/P-H coupling of phenylacetylene with diphenylphosphine oxide under electroreduction conditions using M@SN nanocatalysts.

The nature of the catalyst, as it turned out, is decisive for obtaining a particular product. Monometallic catalyst particles favor the formation of phosphorylated acetylene with triple bond (1) (the yield up to 98%, Table 2, entry 1), while the bimetallic catalyst favors the formation of bisphosphorylated addition adduct with saturated carbon-carbon bonds (2) (Scheme 3, Table S3, entry 1, yield of 95%). Increasing the content of $\text{Ph}_2\text{P}(\text{O})\text{H}$ to 2:1 with respect to phenylacetylene and increasing the amount of electricity passed to 3.5 F makes it possible to obtain a single product (2) with the bimetallic nanocatalysts participation. In the latter case, the reaction is completely atom-economical since there are no formal by-products.



Scheme 3. Comparison of coupling products with mono- and bimetallic catalytic systems (from Table 2 and Table S3).

The poor solubility of product 2 in acetonitrile leads to its precipitation, which prevents the easy separation of catalyst nanoparticles and their reuse after electroreduction of 2. However, in the absence of product 2 the electrolyte solution is transparent, the catalyst is easily separated by centrifugation and can be reused. The contamination of catalyst particles with product 2 can be prevented by heating the mixture to 80 °C or by washing the nanoparticles with chloroform. It has been established that an isolated and regenerated catalyst works without loss of activity at least three times.

Bimetallic catalysts promote the hydrogenation of intermediates, which leads to the final conversion of acetylene into product 2 with saturated C–C bonds. Differences in the activity of mono- and bimetallic catalysts have also been observed previously in numerous works [7,57,58], although the reasons for synergy or fundamentally different selectivity and performance are usually difficult to explain. However, in many cases, the bimetallic catalysts promote reactions accompanied by the hydrogenation of a wide variety of molecules and intermediates, as it is exemplified for iron–cobalt [59,60] or cobalt–copper particles [24,61–65].

It was found that the addition of phenylacetylene, which is electrochemically inactive in the potential working region, to catalyst nanoparticles has a significant effect on voltammograms nanoparticles. Thus, for example, new catalytic peaks appear on the CVs of $\text{Co}^{\text{II}}-\text{SN}_{50}-\text{Cu}^{\text{II}}$ reduction in the presence of phenylacetylene at lower potentials (Figure S9), and a catalytic increase in current is observed when acetylene is added to the $\text{SN}_{50}-\text{Cu}^{\text{II}}$ (Figure S10) and $\text{SN}_{120}-\text{Cu}^{\text{II}}$ (Figure S11) particles. The addition of $\text{Ph}_2\text{P}(\text{O})\text{H}$, which itself is reduced at high potentials ($E_p = -2.89$ V, Figure S12), does not noticeably affect the currents and potentials of the first peaks of catalyst reduction.

The product yields represented in Table 2 indicate the difference in the content of products obtained via the Cu-catalyzed phosphorylation reaction under the use of $\text{SN}_{120}-$

Cu^{II} and $\text{SN}_{50}\text{-Cu}^{\text{II}}$ as nanocatalysts. The specificity of the surfaces of SNs produced via the microemulsion procedure due to the porosity arising from the washing out of the adsorbed TX-100 molecules [53] differentiates $\text{SN}_{50}\text{-Cu}^{\text{II}}$ from $\text{SN}_{120}\text{-Cu}^{\text{II}}$. The more porous surface of $\text{SN}_{50}\text{-Cu}^{\text{II}}$ vs. $\text{SN}_{120}\text{-Cu}^{\text{II}}$ can explain the difference in the yields of products **1** and **2** under their use as nanocatalysts. Thus, nanoparticles SN_{50} provide an optimal basis for both mono and bimetallic nanocatalysts.

Product **2** is easily separated from the reaction mixture since it is poorly soluble in it, and it is sufficient to leave the reaction mixture for some time after the reaction to get almost quantitative precipitation of **2**.

(1-phenylethane-1,2-diyl)bis(diphenylphosphine oxide) (**2**) (CAS Number: 3583-85-5) has practical significance and is produced on an industrial scale by several concerns, for example, BaiFuChem, Xiamen Equation Chemical Co., Ltd. in Uhnshanghai (China) (<http://www.equationchemical.com> (accessed on 31 December 2022), <https://www.baifuchem.com> (accessed on 31 December 2022), <http://www.uhnshanghai.com/uhn/html/20149252096.html> (accessed on 31 December 2022)) as a pharmaceutical intermediate or flame retardant. Thus, we propose a simple and convenient method for the synthesis of this product. Furthermore, this article discussed the different activity and catalytic performance of bimetallic SNs compared to monometallic composites. The synthetic strategies reported here established development of sophisticated and controlled SNs for widespread application.

3. Conclusions

A method is proposed for the preparation of phosphorylation products of terminal acetylene using the example of phenylacetylene and $\text{Ph}_2\text{P}(\text{O})\text{H}$ using a regenerated nanocatalyst based on silica nanoparticles loaded by Cu^{II} , $\text{Co}^{\text{III/II}}$, Fe^{III} via different synthetic techniques in both mono- and bimetallic modes. The synthetic technique has been optimized for controlled cross-coupling of phenylacetylene with retention of the triple bond. Moreover, the use of the bimetallic nanocatalysts allows producing bis-adduct with two phosphine oxide substituents and a fully saturated carbon backbone along with the C-H/P-H cross-coupling of phenylacetylene with retention of the triple bond. Both products are in demand and practically significant. They are obtained in one stage at room temperature by an atom-economical reaction.

Supplementary Materials: The following supporting information can be downloaded at: <https://www.mdpi.com/article/10.3390/ijms24010765/s1>.

Author Contributions: Coordination of manuscript—Y.H.B. and A.R.M.; Preparation of the manuscript—M.V.T. and O.D.B.; Investigation: M.V.T., O.D.B. and T.V.G.; M.V.T. and A.R.M. contributed to the literature review and the writing of the manuscript. All authors have read and agreed to the published version of the manuscript.

Funding: This work was supported by the Russian Science Foundation grant no. 22-13-00017. Authors gratefully acknowledge to Assigned Spectral-Analytical Center of FRC Kazan Scientific Center of RAS for providing necessary facilities to carry out physical-chemical measurements.

Institutional Review Board Statement: Not applicable.

Informed Consent Statement: Not applicable.

Data Availability Statement: All data generated or analyzed during this study are included in this published article; further inquiries can be directed to the corresponding author.

Conflicts of Interest: The authors declare that the research was conducted in the absence of any commercial or financial relationships that could be construed as a potential conflict of interest.

References

1. Sheldon, R.A. Fundamentals of green chemistry: Efficiency in reaction design. *Chem. Soc. Rev.* **2012**, *41*, 1437–1451. [[CrossRef](#)] [[PubMed](#)]
2. Huo, L.-Q.; Shi, L.-L.; Fu, J.-K. Iron–Copper Dual Catalysis Enabling C-C and C-X (X = N, B, P, S, Sn) Bond Formation. *Eur. J. Org. Chem.* **2022**, *2022*, e202200454. [[CrossRef](#)]
3. Gandeepan, P.; Müller, T.; Zell, D.; Cera, G.; Warratz, S.; Ackermann, L. 3d Transition Metals for C–H Activation. *Chem. Rev.* **2019**, *119*, 2192–2452. [[CrossRef](#)] [[PubMed](#)]
4. Nishad, R.C.; Kumar, S.; Rit, A. Hetero- and Homobimetallic Complexes Bridged by a Bis(NHC) Ligand: Synthesis via Selective Sequential Metalation and Catalytic Applications in Tandem Organic Transformations. *Organometallics* **2021**, *40*, 915–926. [[CrossRef](#)]
5. Liu, X.; Wang, D.; Li, Y. Synthesis and catalytic properties of bimetallic nanomaterials with various architectures. *Nano Today* **2012**, *7*, 448–466. [[CrossRef](#)]
6. Pérez-Temprano, M.H.; Casares, J.A.; Espinet, P. Bimetallic Catalysis using Transition and Group 11 Metals: An Emerging Tool for C-C Coupling and Other Reactions. *Chem. Eur. J.* **2012**, *18*, 1864–1884. [[CrossRef](#)]
7. Kim, U.B.; Jung, D.J.; Jeon, H.J.; Rathwell, K.; Lee, S.-g. Synergistic Dual Transition Metal Catalysis. *Chem. Rev.* **2020**, *120*, 13382–13433. [[CrossRef](#)]
8. Lorion, M.M.; Maindan, K.; Kapdi, A.R.; Ackermann, L. Heteromultimetallic catalysis for sustainable organic syntheses. *Chem. Soc. Rev.* **2017**, *46*, 7399–7420. [[CrossRef](#)]
9. Loza, K.; Heggen, M.; Epple, M. Synthesis, Structure, Properties, and Applications of Bimetallic Nanoparticles of Noble Metals. *Adv. Funct. Mater.* **2020**, *30*, 1909260. [[CrossRef](#)]
10. Kalidindi, S.B.; Jagirdar, B.R. Nanocatalysis and Prospects of Green Chemistry. *ChemSusChem* **2012**, *5*, 65–75. [[CrossRef](#)]
11. Dang-Bao, T.; Pla, D.; Favier, I.; Gómez, M. Bimetallic Nanoparticles in Alternative Solvents for Catalytic Purposes. *Catalysts* **2017**, *7*, 207. [[CrossRef](#)]
12. Kim, S.; Muthurasu, A. Metal-organic framework–assisted bimetallic Ni@Cu microsphere for enzyme-free electrochemical sensing of glucose. *J. Electroanal. Chem.* **2020**, *873*, 114356. [[CrossRef](#)]
13. Bochkova, O.; Khrizanforov, M.; Gubaidullin, A.; Gerasimova, T.; Nizameev, I.; Kholin, K.; Laskin, A.; Budnikova, Y.; Sinyashin, O.; Mustafina, A. Synthetic tuning of CoII-doped silica nanoarchitecture towards electro-chemical sensing ability. *Nanomaterials* **2020**, *10*, 1338. [[CrossRef](#)] [[PubMed](#)]
14. Dudkina, Y.B.; Gryaznova, T.V.; Osin, Y.N.; Salnikov, V.V.; Davydov, N.D.; Fedorenko, S.V.; Mustafina, A.R.; Vicic, D.A.; Sinyashin, O.G.; Budnikova, Y.H. Nanoheterogeneous Catalysis in Electrochemically Induced Olefin Perfluoroalkylation. *Dalton Trans.* **2015**, *44*, 8833–8838. [[CrossRef](#)]
15. Fedorenko, S.; Jilkin, M.; Nastapova, N.; Yanilkin, V.; Bochkova, O.; Buriliov, V.; Nizameev, I.; Nasretdinova, G.; Kadirov, M.; Mustafina, A.; et al. Surface decoration of silica nanoparticles by Pd(0) deposition for catalytic application in aqueous solutions. *Colloids Surf. A* **2015**, *486*, 185–191. [[CrossRef](#)]
16. Khrizanforov, M.; Fedorenko, S.V.; Strelkova, S.O.; Kholin, K.V.; Mustafina, A.; Zhilkin, M.Y.; Khrizanforova, V.; Osin, Y.N.; Salnikov, V.V.; Gryaznova, T.; et al. Ni (III) Complex Stabilized by Silica Nanoparticles as an Efficient Nanoheterogeneous Catalyst for Oxidative C-H Fluoroalkylation. *Dalton Trans.* **2016**, *45*, 11976–11982. [[CrossRef](#)]
17. Budnikova, Y. Group VIII Base Metal Nanocatalysts with Encapsulated Structures as an Area of Green Chemistry. *Pet. Chem.* **2017**, *57*, 1259–1276. [[CrossRef](#)]
18. Fedorenko, S.V.; Jilkin, M.E.; Gryaznova, T.V.; Iurko, E.O.; Bochkova, O.D.; Mukhametshina, A.R.; Nizameev, I.R.; Kholin, K.V.; Mazzaro, R.; Morandi, V.; et al. Silica Nanospheres Coated by Ultrasmall Ag0 Nanoparticles for Oxidative Catalytic Application. *Colloid Interface Sci. Commun.* **2017**, *21*, 1–5. [[CrossRef](#)]
19. Khrizanforov, M.N.; Fedorenko, S.V.; Mustafina, A.R.; Kholin, K.V.; Nizameev, I.R.; Strelkova, S.O.; Grinenko, V.V.; Gryaznova, T.V.; Zairov, R.R.; Mazzaro, R.; et al. Silica-Supported Silver Nanoparticles as an Efficient Catalyst for Aromatic C-H Alkylation and Fluoroalkylation. *Dalton Trans.* **2018**, *47*, 9608–9616. [[CrossRef](#)]
20. Budnikova, Y.H.; Bochkova, O.; Khrizanforov, M.; Nizameev, I.; Kholin, K.; Gryaznova, T.; Laskin, A.; Dudkina, Y.; Strelkova, S.; Fedorenko, S.; et al. Selective C(sp²)-H Amination Catalyzed by High-Valent Cobalt(III)/(IV)-bpy Com-plex Immobilized on Silica Nanoparticles. *Chemcatchem* **2019**, *11*, 5615–5624. [[CrossRef](#)]
21. Khrizanforov, M.N.; Fedorenko, S.V.; Mustafina, A.R.; Khrizanforova, V.V.; Kholin, K.V.; Nizameev, I.R.; Gryaznova, T.V.; Grinenko, V.V.; Budnikova, Y.H. Nano-architecture of silica nanoparticles as a tool to tune both electrochemical and catalytic behavior of NiII@SiO₂. *RSC Adv.* **2019**, *9*, 22627–22635. [[CrossRef](#)] [[PubMed](#)]
22. Wang, A.W.; Li, R.; Hua, X.; Zhang, R. Methanol electrooxidation on glassy carbon electrode modified with bimetallic Ni(II)Co(II)salen complexes encapsulated in mesoporous zeolite. *Electrochim. Acta* **2015**, *163*, 48–56. [[CrossRef](#)]
23. Sun, H.; Lin, L.; Hua, W.; Xie, X.; Mu, Q.; Feng, K.; Zhong, J.; Lyu, F.; Deng, Z.; Peng, Y. Atomically dispersed Co–Cu alloy reconstructed from metal-organic framework to promote electrochemical CO₂ methanation. *Nano Res.* **2022**. [[CrossRef](#)]
24. He, C.; Wang, S.; Jiang, X.; Hu, Q.; Yang, H.; He, C. Bimetallic Cobalt–Copper Nanoparticle-Decorated Hollow Carbon Nanofibers for Efficient CO₂ Electroreduction. *Front. Chem.* **2022**, *10*, 904241. [[CrossRef](#)] [[PubMed](#)]
25. Lecerclé, D.; Sawicki, M.; Taran, F. Phosphine-Catalyzed α -P-Addition on Activated Alkynes: A New Route to P–C–P Backbones. *Org. Lett.* **2006**, *8*, 4283–4285. [[CrossRef](#)]

26. Tang, S.; Liu, Y.; Gao, X.; Wang, P.; Huang, P.; Lei, A. Multi-Metal-Catalyzed Oxidative Radical Alkynylation with Terminal Alkynes: A New Strategy for C(sp³)-C(sp) Bond Formation. *J. Am. Chem. Soc.* **2018**, *140*, 6006–6013. [[CrossRef](#)]
27. Jiang, W.-Q.; Allan, G.; Chen, X.; Fiordeliso, J.J.; Linton, O.; Tannenbaum, P.; Xu, J.; Zhu, P.-F.; Gunnet, J.; Demarest, K.; et al. Novel phosphorus-containing 17 β -side chain mifepristone analogues as progesterone receptor antagonists. *Steroids* **2006**, *71*, 949–954. [[CrossRef](#)] [[PubMed](#)]
28. Castoldi, L.; Rajkiewicz, A.A.; Olofsson, B. Transition metal-free and regioselective vinylation of phosphine oxides and H-phosphinates with VBX reagents. *Chem. Commun.* **2020**, *56*, 14389–14392. [[CrossRef](#)]
29. Guo, H.-M.; Zhou, Q.-Q.; Jiang, X.; Shi, D.-Q.; Xiao, W.-J. Catalyst- and Oxidant-Free Desulfonative C-P Couplings for the Synthesis of Phosphine Oxides and Phosphonates. *Adv. Synth. Catal.* **2017**, *359*, 4141–4146. [[CrossRef](#)]
30. Afanasiev, V.V.; Beletskaya, I.P.; Kazankova, M.A.; Efimova, I.V.; Antipin, M.U. A Convenient and Direct Route to Phosphinoalkynes via Copper-Catalyzed Cross-Coupling of Terminal Alkynes with Chlorophosphanes. *Synthesis* **2003**, *18*, 2835–2838. [[CrossRef](#)]
31. Liu, L.; Wu, Y.; Wang, Z.; Zhu, J.; Zhao, Y. Mechanistic Insight into the Copper-Catalyzed Phosphorylation of Terminal Alkynes: A Combined Theoretical and Experimental Study. *J. Org. Chem.* **2014**, *79*, 6816–6822. [[CrossRef](#)] [[PubMed](#)]
32. Chen, C.C.; Waser, J. Room temperature alkynylation of H-phosphi(na)tes and secondary phosphine oxides with ethynylbenziodoxolone (EBX) reagents. *Chem. Commun.* **2014**, *50*, 12923–12926. [[CrossRef](#)] [[PubMed](#)]
33. Kondoh, A.; Yorimitsu, H.; Oshima, K. 1-Alkynylphosphines and Their Derivatives as Key Starting Materials in Creating New Phosphines. *Chem. Asian J.* **2010**, *5*, 398–409. [[CrossRef](#)]
34. Arisawa, M.; Onoda, M.; Hori, C.; Yamaguchi, M. Copper-Catalyzed C-P Coupling of 1-alkynylphosphine oxides from 1-alkynes and tetraphenylbiphosphine. *Tetrahedron Lett.* **2006**, *47*, 5211–5213. [[CrossRef](#)]
35. Hu, J.; Zhao, N.; Yang, B.; Wang, G.; Guo, L.-N.; Liang, Y.-M.; Yang, S.-D. Copper-Catalyzed C-P Coupling through Decarboxylation. *Chem. Eur. J.* **2011**, *17*, 5516–5521. [[CrossRef](#)] [[PubMed](#)]
36. Hu, G.; Gao, Y.; Zhao, Y. Copper-Catalyzed Decarboxylative C-P Cross-Coupling of Alkynyl Acids with H-Phosphine Oxides: A Facile and Selective Synthesis of (E)-1-Alkenylphosphine Oxides. *Org. Lett.* **2014**, *16*, 4464–4467. [[CrossRef](#)] [[PubMed](#)]
37. Ruan, H.; Meng, L.-G.; Xu, H.; Liang, Y.; Wang, L. Additive-free coupling of bromoalkynes with secondary phosphine oxides to generate alkynylphosphine oxides in acetic anhydride. *Org. Biomol. Chem.* **2020**, *18*, 1087–1090. [[CrossRef](#)]
38. Wang, Y.; Gan, J.; Liu, L.; Yuan, H.; Gao, Y.; Liu, Y.; Zhao, Y. Cs₂CO₃-Promoted One-Pot Synthesis of Alkynylphosphonates, -phosphinates, and -phosphine Oxides. *J. Org. Chem.* **2014**, *79*, 3678–3683. [[CrossRef](#)]
39. Yang, J.; Chen, T.; Zhou, Y.; Yin, S.; Han, L.-B. Palladium-catalyzed dehydrogenative coupling of terminal alkynes with secondary phosphine oxides. *Chem. Commun.* **2015**, *51*, 3549–3551. [[CrossRef](#)]
40. Wang, T.; Chen, S.; Shao, A.; Gao, M.; Huang, Y.; Lei, A. Silver-Mediated Selective Oxidative Cross-Coupling between C-H/P-H: A Strategy to Construct Alkynyl(diaryl)phosphine Oxide. *Org. Lett.* **2015**, *17*, 118–121. [[CrossRef](#)]
41. Gérard, P.; Veillard, R.; Alayrac, C.; Gaumont, A.-C.; Evano, G. Room-Temperature Alkynylation of Phosphine Oxides with Copper Acetylides: Practical Synthesis of Alkynylphosphine Oxides. *Eur. J. Org. Chem.* **2016**, *2016*, 633–638. [[CrossRef](#)]
42. Zhang, J.-Q.; Chen, T.; Zhang, J.-S.; Han, L.-B. Silver-Free Direct Synthesis of Alkynylphosphine Oxides via spC-H/P(O)-H Dehydrogenative Coupling Catalyzed by Palladium. *Org. Lett.* **2017**, *19*, 4692–4695. [[CrossRef](#)] [[PubMed](#)]
43. King, A.K.; Gallagher, K.J.; Mahon, M.F.; Webster, R.L. Markovnikov versus anti-Markovnikov Hydrophosphination: Divergent Reactivity Using an Iron(II) b-Diketiminato Pre-Catalyst. *Chem. Eur. J.* **2017**, *23*, 9039–9043. [[CrossRef](#)] [[PubMed](#)]
44. Chen, T.; Zhao, C.-Q.; Han, L.-B. Hydrophosphorylation of Alkynes Catalyzed by Palladium: Generality and Mechanism. *J. Am. Chem. Soc.* **2018**, *140*, 3139–3155. [[CrossRef](#)]
45. Ikeshita, D.; Masuda, Y.; Ishida, N.; Murakami, M. Photoinduced Hydrophosphination of Terminal Alkynes with Tri(o-tolyl)phosphine: Synthesis of Alkenylphosphonium Salts. *Org. Lett.* **2022**, *24*, 2504–2508. [[CrossRef](#)]
46. Trostyanskaya, I.G.; Beletskaya, I.P. Copper (II)-catalyzed regio- and stereoselective addition of H/P(O)R₂ to alkynes. *Tetrahedron* **2014**, *70*, 2556–2562. [[CrossRef](#)]
47. Khemchyan, L.L.; Ivanova, J.V.; Zalesskiy, S.S.; Ananikov, V.P.; Beletskaya, I.P.; Starikova, Z.A. Unprecedented Control of Selectivity in Nickel-Catalyzed Hydrophosphorylation of Alkynes: Efficient Route to Mono and Bisphosphonates. *Adv. Synth. Catal.* **2014**, *356*, 771–780. [[CrossRef](#)]
48. Chen, X.; Li, X.; Chen, X.-L.; Qu, L.-B.; Chen, J.-Y.; Sun, K.; Zhao, Y.-F. A one-pot strategy to synthesize β -ketophosphonates: Silver/copper catalyzed direct oxyphosphorylation of alkynes with H-phosphonates and oxygen in the air. *Chem. Commun.* **2015**, *51*, 3846–3849. [[CrossRef](#)]
49. Zhang, J.-S.; Zhang, J.-Q.; Chen, T.; Han, L.-B. t-BuOK-mediated reductive addition of P(O)-H compounds to terminal alkynes forming β -arylphosphine oxides. *Org. Biomol. Chem.* **2017**, *15*, 5462–5467. [[CrossRef](#)]
50. Gao, Y.; Wang, G.; Chen, L.; Xu, P.; Zhao, Y.; Zhou, Y.; Han, L.-B. Copper-Catalyzed Aerobic Oxidative Coupling of Terminal Alkynes with H-Phosphonates Leading to Alkynylphosphonates. *J. Am. Chem. Soc.* **2009**, *131*, 7956–7957. [[CrossRef](#)]
51. Song, W.-Z.; Li, J.-H.; Li, M.; He, J.-N.; Dong, K.; Ullah, K.; Zheng, Y.-B. Copper-catalyzed one-pot synthesis of alkynylphosphonates. *Synth. Commun.* **2019**, *49*, 697–703. [[CrossRef](#)]
52. Shen, J.; Xiao, B.; Hou, Y.; Wang, X.; Li, G.-Z.; Chen, J.-C.; Wang, W.-L.; Cheng, J.-B.; Yang, B.; Yang, S.-D. Cobalt(II)-Catalyzed Bisfunctionalization of Alkenes with Diarylphosphine Oxide and Peroxide. *Adv. Synth. Catal.* **2019**, *361*, 5198–5209. [[CrossRef](#)]

53. Mukhametshina, A.R.; Fedorenko, S.V.; Zueva, I.V.; Petrov, K.A.; Masson, P.; Nizameev, I.R.; Mustafina, A.R.; Sinyashin, O.G. Luminescent silica nanoparticles for sensing acetylcholinesterase-catalyzed hydrolysis of acetylcholine. *Biosens. Bioelectron.* **2016**, *77*, 871–878. [[CrossRef](#)] [[PubMed](#)]
54. Skripacheva, V.; Mustafina, A.; Davydov, N.; Burirov, V.; Konovalov, A.; Soloveva, S.; Antipin, I. Interfacial adsorption and stripping of ions as a reason of stimuli responsive luminescence of Tb-doped silica nanoparticles. *Mater. Chem. Phys.* **2012**, *132*, 488–493. [[CrossRef](#)]
55. Ahkam, Q.M.; Khan, E.U.; Iqbal, J.; Murtaza, A.; Khan, M.T. Synthesis and characterization of cobalt-doped SiO₂ nanoparticles. *Phys. B Condens. Matter* **2019**, *572*, 161–167. [[CrossRef](#)]
56. Nicholls, D. Electronic spectra of transition-metal complexes. In *Complexes and First-Row Transition Elements*; Palgrave: London, UK, 1974; pp. 73–99. [[CrossRef](#)]
57. Bhol, P.; Bhavya, M.B.; Swain, S.; Saxena, M.; Samal, A.K. Modern Chemical Routes for the Controlled Synthesis of Anisotropic Bimetallic Nanostructures and Their Application in Catalysis. *Front. Chem.* **2020**, *8*, 357. [[CrossRef](#)] [[PubMed](#)]
58. Sharma, G.; Kumar, A.; Sharma, S.; Naushad, M.; Dwivedi, R.P.; AlOthman, Z.A.; Mola, G.T. Novel development of nanoparticles to bimetallic nanoparticles and their composites: A review. *J. King Saud Univ.-Sci.* **2019**, *31*, 257–269. [[CrossRef](#)]
59. Li, K.; Li, Y.; Peng, W.; Zhang, G.; Zhang, F.; Fan, X. Bimetallic Iron–Cobalt Catalysts and Their Applications in Energy-Related Electrochemical Reactions. *Catalysts* **2019**, *9*, 762. [[CrossRef](#)]
60. Rai, R.K.; Al Maksoud, W.; Morlanés, N.; Harb, M.; Ahmad, R.; Genovese, A.; Hedhili, M.N.; Cavallo, L.; Basset, J.-M. Iron–Cobalt-Based Materials: An Efficient Bimetallic Catalyst for Ammonia Synthesis at Low Temperatures. *ACS Catal.* **2022**, *12*, 587–599. [[CrossRef](#)]
61. Xiang, Y.; Kruse, N. Cobalt–copper based catalysts for higher terminal alcohols synthesis via Fischer–Tropsch reaction. *J. Energy Chem.* **2016**, *25*, 895–906. [[CrossRef](#)]
62. Ge, X.; Sun, H.; Dong, K.; Tao, Y.; Wang, Q.; Chen, Y.; Zhang, G.; Cui, P.; Wang, Y.; Zhang, Q. Copper–cobalt catalysts supported on mechanically mixed HZSM-5 and g-Al₂O₃ for higher alcohols synthesis via carbon monoxide hydrogenation. *RSC Adv.* **2019**, *9*, 14592–14598. [[CrossRef](#)] [[PubMed](#)]
63. Srivastava, S.; Jadeja, G.C.; Parikh, J. A versatile bi-metallic copper–cobalt catalyst for liquid phase hydrogenation of furfural to 2-methylfuran. *RSC Adv.* **2016**, *6*, 1649–1658. [[CrossRef](#)]
64. Zhang, Q.; Zuo, J.; Wang, L.; Peng, F.; Chen, S.; Liu, Z. Non Noble-Metal Copper–Cobalt Bimetallic Catalyst for Efficient Catalysis of the Hydrogenolysis of 5-Hydroxymethylfurfural to 2,5-Dimethylfuran under Mild Conditions. *ACS Omega* **2021**, *6*, 10910–10920. [[CrossRef](#)]
65. Call, A.; Casadevall, C.; Acuña-Parés, F.; Casitas, A.; Lloret-Fillol, J. Dual cobalt–copper light-driven catalytic reduction of aldehydes and aromatic ketones in aqueous media. *Chem. Sci.* **2017**, *8*, 4739–4749. [[CrossRef](#)] [[PubMed](#)]
66. Chen, Y.-X.; Zhang, M.; Zhang, S.-Z.; Hao, Z.-Q.; Zhan, Z.-H. Copper-decorated covalent organic framework as a heterogeneous photocatalyst for phosphorylation of terminal alkynes. *Green Chemistry* **2022**, *24*, 4071–4081. [[CrossRef](#)]
67. Guo, H.; Yoshimura, A.; Chen, T.; Saga, Y.; Han, L.-B. Air-induced double addition of P(O)–H bonds to alkynes: A clean and practical method for the preparation of 1,2-bisphosphorylethanes. *Green Chemistry* **2017**, *19*, 1502–1506. [[CrossRef](#)]

Disclaimer/Publisher’s Note: The statements, opinions and data contained in all publications are solely those of the individual author(s) and contributor(s) and not of MDPI and/or the editor(s). MDPI and/or the editor(s) disclaim responsibility for any injury to people or property resulting from any ideas, methods, instructions or products referred to in the content.